Journal of Applied Polymer Science

# Sensitivity of PMMA nanoindentation measurements to strain rate

**Tao Jin,[1] Zhiwei Zhou,[2] Zhenguo Liu,[1] Gesheng Xiao,[1] Guozheng Yuan,[1] Xuefeng Shu[1]**

[1]Institute of Applied Mechanics and Biomedical Engineering, Taiyuan University of Technology, Taiyuan 030024, China

[2]State Key Laboratory of Frozen Soil Engineering, Cold and Arid Regions Environmental and Engineering Research Institute, Chinese Academy of Sciences, Lanzhou 730000, China

Correspondence to: X. Shu (E-mail: shuxuefeng@tyut.edu.cn)

**ABSTRACT:** This study aims to investigate the effects of strain rate on polymethyl methacrylate (PMMA) nanoindentation measurements. Nanoindentation experiments were used to characterize the mechanical properties of PMMA. A wide range of strain rates were employed to examine strain rate sensitivity of PMMA. The test results indicate that the elastic modulus and hardness of PMMA are strain-rate-dependent. In addition, both the elastic modulus and hardness of PMMA exhibit increases with increasing strain rate. However, the elastic modulus became a stable value until strain-rate of 0.2 $s^{-1}$. Creep behavior of PMMA under the condition of high strain rate is more obvious than that experience a low strain rate. Moreover, the effects of strain rate on the PMMA nanomechanical properties are detailed analyzed by discussing each stage of the indentation process. © 2015 Wiley Periodicals, Inc. J. Appl. Polym. Sci. **2015**, *132*, 41896.

**KEYWORDS:** amorphous; mechanical properties; viscosity and viscoelasticity

Received 7 September 2014; accepted 18 December 2014

**DOI: 10.1002/app.41896**

## INTRODUCTION

PMMA is one of the most frequently employed materials used in various fields for instance in aerospace and automotive industry.[1–3] An overall understanding of the mechanical properties of PMMA is required for the design and application in industry. Therefore, there are many investigations about the mechanical responses of PMMA through various test methods.[4–9] However, PMMA is often suffered a wide range of loading conditions such as strain rate in its practical application. Hence, numbers of researchers focus on the mechanical behavior of PMMA in terms of strain rate sensitivity and many corresponding experimental studies have been carried out.[3,6,7] Nonetheless, the sensitivity of PMMA nanomechanical to strain rate is still required an overall understood. In this case, nanoindentation is a very powerful tool for studying the mechanical responses on a micro- and nanoscale level and provides accurate consecutive measurements of the indentation load ($P$) and penetration depth ($h$).[2,10–14] Nanoindentation is a method of testing the mechanical properties of a material such as hardness and Young's modulus on the microscopic scale.[15] In conventional nanoindentation, a small tip is pressed into a sample with a known load (force) and retracted sequentially, which generates a force–displacement curve.[16] The mechanical properties, elastic modulus, and hardness can be obtained from the results of nanoindentation analysis.[15–19] The indentation procedure developed by Oliver and Pharr[15] has been widely used for polymeric materials such as PMMA. Many investigations have been reported to describe the nanoindentation test on PMMA. Mukherjee[2] studied the indentation hardness of PMMA and ZnO nanoparticle-reinforced PMMA. Hochstetter[20] made an attempt to identify the true material stress/strain curves of PMMA from nanoindentation experiments by using nonself similar tip shapes. Some comparative analysis on the nanoindentation of PMMA and some other polymers were proposed by Lee.[16] Peng *et al.*[21] studied the shear creep compliance of PMMA by instrumented indentation. Giró-Paloma[22] tested a wide range of thermoplastic polymer materials, including glassy and semicrystalline polymers, using instrumented indentation to the study of the mechanical properties of polymers. Menncík *et al.*[23] changed the holding time to obtain the viscoelastic parameters from the creep data as well as elastic modulus and hardness of PMMA. Additionally, given the loading conditions in practical application of polymers, Oyen[17] applied different load levels and loading rates to investigate sensitivity of polymer nanoindentation creep measurements to experimental variables. However, there is little work about the understanding of how the strain rate affects the nanomechanical properties of PMMA. Accordingly, nanoindentation is employed in the present paper to study the effects of strain rate on PMMA nanomechanical properties.

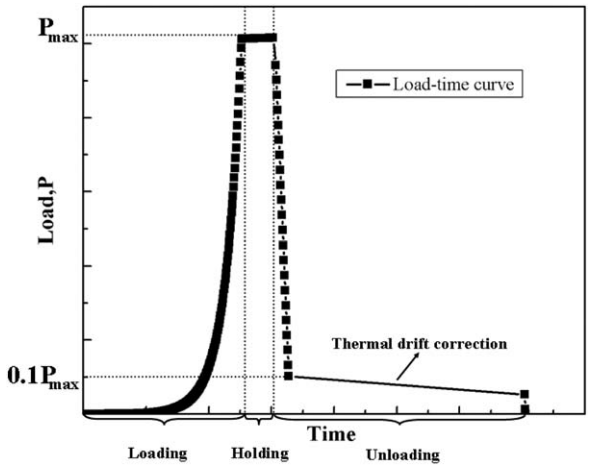


**Figure 1.** Schematic load–time (P–t) input function for CSM indentation tests.

## EXPERIMENTAL

Nanoindentation tests were performed using a Nano-indenter G200 test system produced by Agilent Technologies. The triangular pyramid Berkovich diamond indenter was employed. Material tested in this investigation was 5-mm-thick sheet of PMMA polymers (polymethyl methacrylate). Commercial grade of the material was purchased from a supplier under the trade names, Degussa AG Plexiglas® PMMA. According to the supplier, the PMMA sheet with number-average molecular weight ($M_n$) and glass transition temperature ($T_g$) of 22,000 g/mol and 105°C, respectively. The PMMA sheet is produced through a traditional cell cast method, and thus, no molecular chain orientation exists in the as-cast sheet. In order to study the sensitivity of PMMA nanoindentation measurements to strain rate, the continuous stiffness measurement (CSM) technique was employed to the nanoindentation tests. The indentation tests were carried out at seven strain rates of 0.01, 0.03, 0.05, 0.1, 0.2, 0.3, and 0.5 $s^{-1}$. In addition, an additional harmonic movement with an amplitude of 2 nm and a driving frequency of 45 Hz was applied on the indenter based on the CSM technique. The maximum indentation depth was set to be 2000 nm. As shown in Figure 1, the indenter remained at the corresponding peak load for 10 s as long as the maximum indentation depth achieved in order to release creep deformation. After that, the load dropped to 0.1Pmax for thermal drift correction and then to zero during the unloading stage. In addition, the loading stage is strain-rate control part and the holding stage is creep part. The mean value of CSM measurement data for hardness and elastic modulus between 500 and 1900 nm was taken as a single measurement result to avoid the indentation size effects. Moreover, each test was performed at room temperature (25°C) and repeated three to four times. Furthermore, the mean value of elastic modulus and hardness were used for the following discussion.

## RESULTS AND DISCUSSION

Typical load-displacements curves of PMMA indented under different strain rates are shown in Figure 2. The indents were chosen to have the same displacement, in order to enable a better visual comparison. Increasing load was required to reach the same indentation displacement as strain rate increases, indicating the strain rate sensitivity of PMMA. This phenomenon is related to the existence of viscous deformation during the ramp time. At a low strain rate, the ramp time is longer than that at a high strain rate as shown in Figure 3. Consequently, viscous deformation is largely exhausted during the loading results in a deeper indentation depth. However, viscous deformation cannot be released fully during the loading under a high strain rate condition. Therefore, with the increasing strain rate, load required to reach the same indentation depth increases obviously. In addition, many details about the indentation test results analysis are given elsewhere.[17,19] Based on the CSM technique, the contact stiffness $S$ can be calculated from eq. (1):[17]

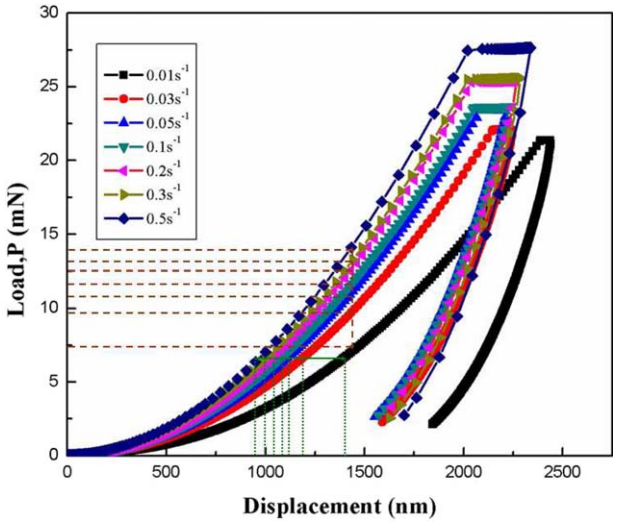


**Figure 2.** Typical recording of load versus displacement during indentation tests under different strain-rates. [Color figure can be viewed in the online issue, which is available at wileyonlinelibrary.com.]

$$S = \left[\frac{1}{\frac{F_{amp}}{h_{amp}}\cos\varphi - (K_s - m\omega^2)} - \frac{1}{K_f}\right]^{-1} \quad (1)$$

where $F_{amp}$ is the amplitude of harmonic excitation force; $h_{amp}$,

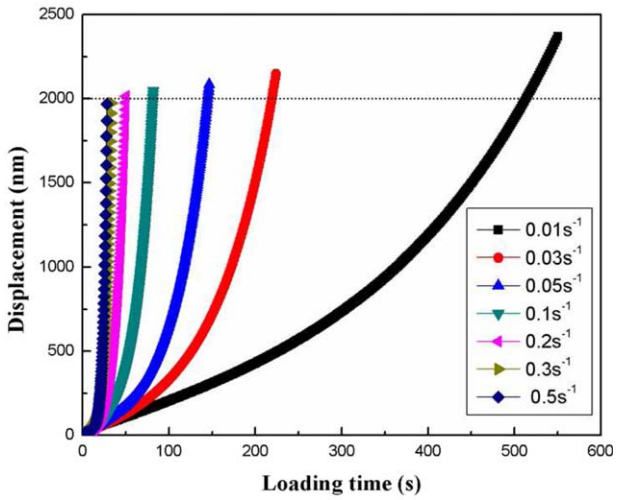


**Figure 3.** The record of displacement-loading time during loading stage. [Color figure can be viewed in the online issue, which is available at wileyonlinelibrary.com.]

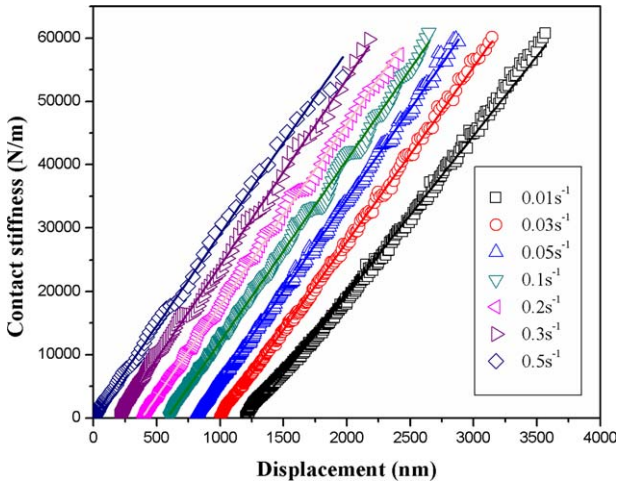


**Figure 4.** Contact stiffness of PMMA under different strain rates plotted against displacement (Some curves are parallelly moved for a clear visual comparison and the solid lines are corresponding linear fitting results). [Color figure can be viewed in the online issue, which is available at wileyonlinelibrary.com.]

the response displacement amplitude (~2 nm); $\varphi$, the phase shift that harmonic displacement lags behind the harmonic excitation force; $\omega = 2\pi f$, the angular frequency ($f = 45$ Hz); $K_s$, the spring constant in the vertical direction; $K_f$, frame stiffness; and $m$ is the mass of compression bar connected to the indenter.

Therefore, the contact stiffness of PMMA under the loading with different strain rates can be obtained. As shown in Figure 4, the contact stiffness increases linearly with the displacement increasing. Additionally, the slopes of the fitting results are 25.12, 27.65, 28.65, 28.69, 28.66, 29.47, and 28.9 N $m^{-1}$ $nm^{-1}$ for different loading strain rates of 0.01, 0.03, 0.05, 0.1, 0.2, 0.3, and 0.5 $s^{-1}$, respectively. It exhibits increase as strain rate increases and then become stable, which results in the variation in elastic modulus. In this study, a perfect Berkovich diamond indenter was used. Hence, the projected contact area is calculated as follows:

$$A_c = 24.56 h_c^2 \tag{2}$$

where $h_c$ is the contact depth and can be calculated as follows:

$$h_c = h - \varepsilon \frac{P}{S} \tag{3}$$

where $\varepsilon = 0.75$ is a constant for the Berkovich indenter. Then, the hardness can be obtained by the following:

$$H = \frac{P}{A_c} \tag{4}$$

where $P$ is the contact load, the elastic modulus of the indented material is obtained from the following eq. (5):[17]

$$\frac{1}{E_r} = \frac{1 - \nu^2}{E} + \frac{1 - \nu_i^2}{E_i} \tag{5}$$

where $E_i$, $\nu_i$ are the modulus and Poisson's ratio of the indenter tip (diamond), $E$, $\nu$ are the modulus and Poisson's ratio of the indented material and $E_r$ is the reduced elastic modulus. Sneddon's stiffness equation provides the foundational relationship between reduced elastic modulus ($E_r$), ($S$), and contact area ($A_c$):

$$E_r = \frac{\sqrt{\pi}}{2\beta} \frac{S}{\sqrt{A_c}} \tag{6}$$

where $\beta = 1.034$ is the shape constant of Berkovich tip. Consequently, the elastic modulus and hardness of indented material can be acquired. As shown in Figure 5(a), both the elastic modulus and hardness of PMMA under different strain rates become a stable value as indent displacement increases indicating that the indention size almost has no effect on the measurements. Additionally, a high strain rate results in a higher elastic modulus, which can be attributed to that a high strain rate causing larger contact stiffness as analyzed above. Moreover, the hardness of PMMA also increases with the increasing strain rate which is described detailed in Figure 5(b). Figure 5(b) shows

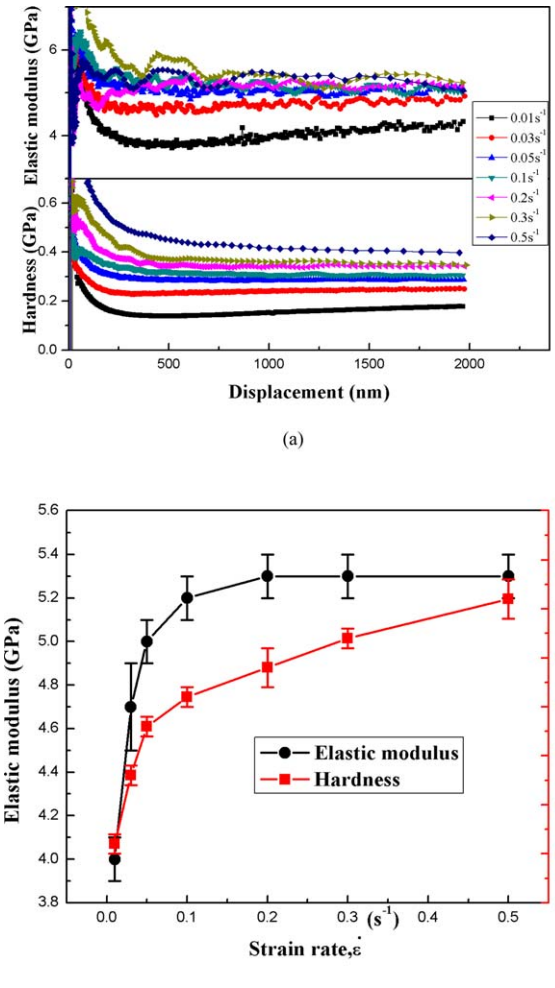


**Figure 5.** Elastic modulus-displacement curves and hardness-displacement curves of PMMA (b); Elastic modulus and hardness of PMMA as a function of strain rate (b). [Color figure can be viewed in the online issue, which is available at wileyonlinelibrary.com.]

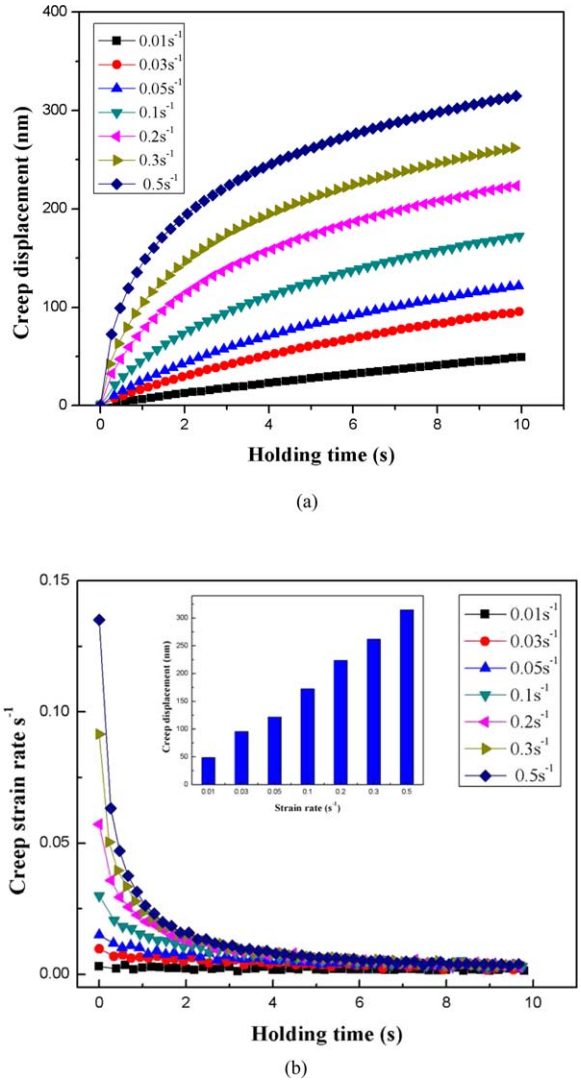


**Figure 6.** Creep displacement (a) and indentation strain rate (b) during the holding stage under different strain rates. [Color figure can be viewed in the online issue, which is available at wileyonlinelibrary.com.]

the elastic modulus and hardness of PMMA as a function of strain rate. The elastic modulus is rate-dependent for PMMA which exhibits increase as the strain rate increases until 0.2 $s^{-1}$ in accordance with the contact stiffness. On the other hand, the indentation displacement decreases as strain rate increases when applied the same load during the loading stage as shown in Figure 2. Hence, it is easy to infer that the elastic modulus of PMMA increases as the strain rate increases through eqs. (1) (2), (3), (5), and (6). But the difference of the contact stiffness and indentation depth get weaken as strain rates larger enough which is corresponding to the modulus exhibit a stable value when strain above 0.2 $s^{-1}$. When the strain rate is under 0.2 $s^{-1}$, the fluctuation in elastic modulus caused by the strain rate reaches 24.5% [shown as Figure 5(b)]. However, the viscous deformation cannot exhaust fully when the loading rate exceeds 0.2 $s^{-1}$. Under this condition, the hardness of nanoindentation exhibits an increasing value with increasing strain rate, as displayed in Figure 5(b). As described in the previous section, increasing load was required to reach the same indentation displacement as strain rate increases which results in the increase in hardness.

For a viscoelastic material, the creep behavior is also important. Therefore, the mechanical properties of PMMA during holding stage are discussed in present paper. Furthermore, at a high strain rate, more viscous deformation will be accumulated after loading stage, transforming into larger creep deformation during the holding stage as plotted in Figure 6(a). Figure 6(b) plots the relationship between creep strain rate and holding time under different strain rates. The indentation creep strain rate can be calculated as follows:[13]

$$\dot{\varepsilon} = \frac{1}{h}\frac{dh}{dt} \tag{7}$$

where $h$ is the instantaneous indentation depth, and $t$ is time. It is observed that the indentation creep strain rate at the initial holding stage decreases with the decreasing strain rate. At a higher loading rate, the creep strain rate drops quickly at the beginning of the holding stage and then becomes a stable value. The viscous deformation during the loading stage leads to this phenomenon. A higher strain rate leads to a smaller loading time. Hence, more accumulated viscous deformation need to be released at the holding stage, resulting in a higher creep strain rate at the beginning of the holding stage. Hence, a high strain rate corresponds to a large creep deformation.

Figure 7 shows the nanoindentation unloading curves for PMMA under strain rates of 0.01, 0.03, and 0.05 $s^{-1}$. The indentation displacement continues to increase after the holding stage which resulting in the phenomenon of "bulge" when unloading rate is sufficiently low. For strain rates of 0.01, 0.03, and 0.05 $s^{-1}$, the corresponding unloading rates are 0.12, 0.20, and 0.24 mN/s, respectively. Furthermore, it can be observed that the "bulge" phenomenon get weaken as unloading rate increases, indicating the unloading rate dependence of "bulge" phenomenon.

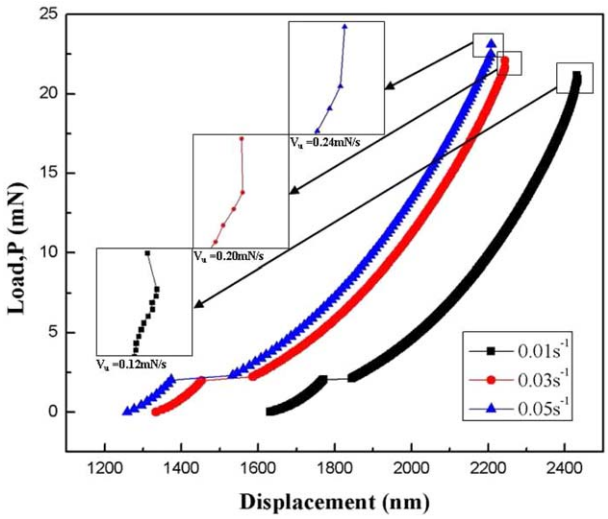


**Figure 7.** Nanoindentation unloading curves for PMMA under strain rates of 0.01$s^{-1}$, 0.03$s^{-1}$ and 0.05$s^{-1}$. [Color figure can be viewed in the online issue, which is available at wileyonlinelibrary.com.]

## CONCLUSIONS

A wide range of strain rates have been employed to examine the sensitivity of the mechanical properties of PMMA to the strain rate. Both the elastic modulus and the hardness are exhibit strain rate-dependent, increasing as strain rate increases. In addition, the viscous deformation occurs throughout the indentation process, which results in the sensitivity of PMMA nanoindentation measurements to strain rate. Furthermore, the existence of "bulge" phenomenon and negative initial unloading stiffness will lead to the inaccuracy of PMMA nanoindentation measurement. Consequently, it is reasonable to test PMMA using CSM technique.

## ACKNOWLEDGMENTS

This study is supported by the National Natural Science Foundation of China (Grant No.11172195). The financial contribution is gratefully acknowledged.

## REFERENCES

1. Zhou, Z. W.; Su, B. Y.; Wang, Z. H.; Li, Z. Q.; Shu, X. F.; Zhao, L. M. *Mater. Lett.* **2013**, *109*, 151.
2. Chakraborty, H.; Sinha, A.; Mukherjee, N.; Ray, D.; Chattopadhyay, P. P. *Mater. Lett.* **2013**, *93*, 137.
3. Nasraoui, M.; Forquin, P.; Siad, L.; Rusinek, A. *Mater. Design.* **2012**, *37*, 500.
4. Wu, H. Y.; Ma, G.; Xia, Y. M. *Mater. Lett.* **2004**, *58*, 3681.
5. Gomez, F. J; Elices, M; Planas, J. *Eng. Fract. Mech.* **2005**, *72*, 1268.
6. Arruda, E. M.; Boyce, M. C.; Jayachandran, R. *Mech. Mater.* **1995**, *19*, 193.
7. Li, Z. H.; Lambros, J. *Int. J. Solids. Struct.* **2001**, *38*, 3549.
8. Nasraoui, M; Forquin, P; Siad, L; Rusinek, A; Dossou, E. Mechanical Behaviour of PMMA: Influence of Temperature and Confining Pressure. In: 9th International Conference On the Mechanical and Physical Behaviour of Materials Under Dynamic Loading, Brussels, Belgium, **2009**.
9. Tham, W. L.; Chow, W. S.; Mohd Ishak, Z. A. *J. Appl. Polym. Sci.* **2010**, *118*, 218.
10. Hodzic, A.; Kim, J. K.; Stachurski, Z. H. *Polymer* **2001**, *42*, 5701.
11. Coleman, J. N; Barron, V; Hedicke, K; Blau, W. J. *Appl. Phys. Lett.* **2002**, *81*, 5123.
12. Lee, S. H.; Wang, S.; Pharr, G. M.; Xu, H. *Compos. A* **2007**, *38*, 1517.
13. Dutta, A. K.; Penumadu, D.; Files, B. *J. Mater. Res.* **2004**, *19*, 158.
14. Tweedie, C. A; Anderson, D. G; Langer, R; Van Vliet, K. J. *Adv. Mater.* **2005**, *17*, 2599.
15. Oliver, W. C; Pharr, G. M. J. *Mater. Res.* **1992**, *7*, 1564.
16. Jee, A. Y.; Lee, M. Y. *Polym. Test.* **2010**, *29*, 95.
17. Oyen, M. L. *Acta Mater.* **2007**, *55*, 3633.
18. Lin, Y. C; Weng, Y. J; Pen, D. J; Li, H. C. *Mater. Design.* **2009**, *30*, 1643.
19. Tsui, T. Y.; Oliver, W. C.; Pharr, G. M. *J. Mater. Res.* **1996**, *11*, 752.
20. Hochstetter, G.; Jimenez, A.; Cano, J. P.; Felder, E. *Tribol. Int.* **2003**, *36*, 973.
21. Peng, G. J; Zhang, T. H; Feng, Y. H; Huan, Y. *Polym. Test.* **2012**, *31*, 1038.
22. Giró-Paloma, J; Roa, J. J; Díez-Pascual, A. M; Rayón, E; Flores, A; Martínez, M; Chimenos, J. M; Fernández, A. I. *Eur. Polym. J.* **2013**, *49*, 4047.
23. Menncík, J; He, L. H; Nemecek, J. *Polym. Test.* **2011**, *30*, 101.